Journal of Immunological Methods 527 (2024) 113641

Contents lists available at ScienceDirect

Journal of Immunological Methods

journal homepage: www.elsevier.com/locate/jim

Comparative assessment of cytometry by time-of-flight and full spectral flow cytometry based on a 33-color antibody panel

Antonia Schäfer [a], Sènan Mickael D'Almeida [b,1], Julien Dorier [c,d], Nicolas Guex [c,d], Jean Villard [a,*], Miguel Garcia [b]

[a] Transplantation Immunology Unit and National Reference Laboratory for Histocompatibility, Geneva University Hospitals, Geneva, Switzerland
[b] Flow Cytometry Core Facility, School of Life Sciences, Ecole Polytechnique Fédérale de Lausanne (EPFL), Lausanne, Switzerland
[c] Bioinformatics Competence Center, University of Lausanne, Lausanne, Switzerland
[d] Bioinformatics Competence Center, Ecole Polytechnique Fédérale de Lausanne (EPFL), Lausanne, Switzerland

ARTICLE INFO

Keywords:
Mass cytometry
Full spectral flow cytometry
Clinical studies
High-dimensional analysis
Natural killer cells

ABSTRACT

Mass cytometry and full spectrum flow cytometry have recently emerged as new promising single cell proteomic analysis tools that can be exploited to decipher the extensive diversity of immune cell repertoires and their implication in human diseases. In this study, we evaluated the performance of mass cytometry against full spectrum flow cytometry using an identical 33-color antibody panel on four healthy individuals. Our data revealed an overall high concordance in the quantification of major immune cell populations between the two platforms using a semi-automated clustering approach. We further showed a strong correlation of cluster assignment when comparing manual and automated clustering. Both comparisons revealed minor disagreements in the quantification and assignment of rare cell subpopulations. Our study showed that both single cell proteomic technologies generate highly overlapping results and substantiate that the choice of technology is not a primary factor for successful biological assessment of cell profiles but must be considered in a broader design framework of clinical studies.

1. Introduction

Fundamental and clinical immunology research is highly dependent on the development and application of single-cell technologies to unravel the complexity of immune cell compartment. Over the past ten years, two innovative single cell proteomic platforms have emerged as new powerful research tools mitigating the number of markers that can be analyzed simultaneously by conventional flow-cytometry due to spectral overlap (Roederer, 2001) and fulfilling the need for high dimensional analysis. Through the utilization of antibodies coupled to metal isotopes, cytometry by time-of-flight or mass cytometry (CyTOF), was the first pioneer technology to enable the simultaneous assessment of up to 50 markers (Bandura et al., 2009; Bendall et al., 2011). The recent advent of a next-generation flow cytometry technique, full spectrum flow cytometry (FSFC), also enables immunophenotyping on a high dimensional scale by the assessment of the full light spectrum emitted by each fluorochrome (Robinson, 2019; Robinson et al., 2015; Robinson et al., 2012; Robinson, 2022) and a subsequent unmixing algorithm discriminating each unique fluorochrome by their specific spectrum (Futamura et al., 2015; Novo et al., 2013; Nolan and Condello, 2013).

These recent technical advancements in the field of single cell proteomics have provided researchers and clinicians with two similar tools to probe the immune system in greater depth. Their availability is a blessing and a curse at the same time, putting researchers and clinicians in front of a considerable challenge when it comes to choosing the appropriate technology. Given their differential technical nature, we aimed to proceed to a comparative study of the biological output of these two technologies – mass cytometry and full spectral flow cytometry – using an identical 33-color antibody panel. We further point out key considerations in the decision-making process for the appropriate modality.

* Corresponding author.
E-mail address: jean.villard@hcuge.ch (J. Villard).
[1] Present address: Viollier AG, Allschwil, Switzerland.

https://doi.org/10.1016/j.jim.2024.113641
Received 22 December 2023; Accepted 12 February 2024
Available online 15 February 2024

2. Material and methods

2.1. Sample preparation

Peripheral blood mononuclear cells (PBMCs) from four different healthy donors were isolated using Ficoll density gradient separation (Gibco). Briefly, whole blood was first diluted with the equal amount of phosphate-buffered saline (PBS) solution, layered onto the Ficoll-Paque (GE healthcare) and centrifuged at 400 x*g* for 20–25 min at 4 °C. Subsequently, PBMCs were isolated from the interface, washed twice with PBS and cryopreserved in fetal calf serum (FCS) supplemented with 10% DMSO. Samples were then stored in liquid nitrogen until use. For the assay, cryopreserved samples were rapidly thawed in a water-bath at 37 °C and washed twice with warm RPMI-1640 (Gibco) supplemented with 10% FCS and – if required – with Pierce Universal Cell Nuclease. Thereafter, cells were counted, equally distributed in 5 ml polypropylene (PP) tubes with a total of 3–4 × 10^6 cells per tube and rested overnight at 37 °C in a medium consisting of RPMI 1640 supplemented with 10% FCS.

2.2. Full spectral flow cytometry

Sample were washed by pelleting with PBS at 400 x *g*. Viability staining was performed by adding 5 µl of a 1:500 diluted ViaDye Red viability staining solution (Cytek®) to the cells and incubated for 20 min at room temperature (RT) in the dark. Cells were subsequently washed with cell staining buffer (CSB). For Fc receptor blocking, cells were blocked with 10 µl of Fc-receptor blocking (Biosciences) solution for 10 min. Thereafter, 70 µl phenotyping antibody cocktail (Table S2) were added to each tube and samples were incubated for another 30 min at 4 °C protected from the light. Following two washes with 2 ml of CSB, cells were fixed and permeabilized for the intracellular staining: To this end, cells were resuspended in 200 µl of Fix/Perm FoxP3 Solution (Foxp3/Transcription Factor Staining Buffer Set, eBiosciences, Thermo Fischer) and left for 20 min at RT in the dark. Cells were then washed twice by pelleting with 2 ml of FoxP3 permeabilization buffer at 800 x *g*. After fixation and permeabilization, 10 µl of intracellular antibody cocktail was added to the cells and incubated for another 30 min at 4 °C protected from the light. Following the incubation time, cells were washed twice by pelleting with 2 ml of CSB, resuspended in a final volume of 400 µl CSB and finally filtered through a 35 µm nylon mesh filter for acquisition. Samples were acquired on a 5-Laser Aurora system (Cytek ®) using the SpectroFlo Software v2.2.0.2. The instrument was subject to daily quality control procedures using SpectroFlo® QC Beads (Lot 2004) as per the manufacturer recommendations.

2.3. Time of flight mass cytometry

Sample were washed by pelleting with PBS at 400 x *g*. Viability staining was performed by resuspending cells in cisplatin viability stain (Fluidigm) at a concentration of 25 µM for 1 min and quenched by adding 5 ml CSB. Cells were subsequently washed with CSB. For Fc receptor blocking, cells were blocked with 10 µl of Fc-receptor blocking (Biosciences) solution for 10 min. Thereafter, 70 µl phenotyping antibody cocktail (Table S1) were added to each tube and samples were incubated for another 30 min at 4 °C. Following two washes with 2 ml of CSB, cells were fixed and permeabilized for the intracellular staining: To this end, cells were resuspended in 200 µl of Fix/Perm FoxP3 Solution (Foxp3/Transcription Factor Staining Buffer Set, eBiosciences, Thermo Fischer) and left for 20 min at RT. Cells were then washed twice by pelleting with 2 ml of FoxP3 permeabilization buffer at 800 x *g*. Prior to the staining, samples were barcoded: each sample to be barcoded was resuspended in 800 µl of barcode permeabilization buffer, simultaneously each barcode was resuspended in 100 µl and finally transferred to the samples. Thereafter, 10 µl of intracellular antibody cocktail was added to the cells and incubated for another 30 min at 4 °C. Following the incubation time, cells were washed twice by pelleting with cell staining buffer, resuspended in 400 µl of intercalator solution containing 1.6% PFA and 0.5 µM iridium-intercalator (Fluidigm) and left at 4 °C overnight. The following day, cells were washed twice by pelleting with 2 ml CSB, followed by two washes with cell acquisition solution. For the acquisition, cells were mixed with EQ calibration beads at a ratio of 1:5, further diluted at 1:10 with cell acquisition buffer and acquired on a CyTOF 2.1 mass cytometry instrument (Standard Biotools).

2.4. Quantification and statistical analysis

The following preprocessing steps were applied to these data sets before further downstream analysis: (i) Spectral unmixing for FSFC data was done using SpectroFlo Software v2.2.0.2 (Cytek ®) (ii) Initial data normalization including beads and debarcoding of the CYTOF data was done using the CyTOF software (Standard Biotools). (iii) Both datasets were then uploaded in FlowJo v.10.7.2 and subject to manual filtering steps on debris and time evolution scale. Thereafter, samples were pregated on single, alive, CD45 + immune cells and exported for downstream analysis.

For the semi-automated analysis, cleaned fcs files from FSFC and CyTOF experiments were loaded and preprocessed using R v4.2.2 (R Core Team, 2022) package flowCore v2.10.0 (Hahne et al., 2009). Data from all samples were concatenated. Raw marker expression values were transformed using inverse hyperbolic sine (asinh) transform with cofactor 5 for CyTOF dataset and 3′000 for FSFC dataset. For each marker, transformed expression values were normalized using a linear transformation to map the 1st and 99th percentiles to 0 and 1 respectively. Clustering was performed with FlowSOM v2.6.0 (Van Gassen et al., 2015) with default parameters used except for the self-organizing map size (xdim = 20, ydim = 20) and the number of clusters for metaclustering (nClus = 30). FlowSOM clustering was performed on the normalized expression values of the following markers: CD3, CD4, CD8a, CD19, CD14, CD56, CD16 and CD57. Clusters were manually assigned to cell populations by inspecting 1D and 2D distribution of marker expression values and grouped to a final of 15 distinct assigned cell populations: CD8+ T cells, CD4+ T cells, CD8+ CD4+ T cells, CD4- CD8- T cells, CD4+ NKT cells, CD8+ NKT cells, CD4- CD8- NKT cells, CD4+ CD8+ NKT cells, CD19+ B cells, CD14+ monocytes, CD56++ NK cells, CD56+ CD16+ CD57- NK cells, CD56+ CD16- CD57- NK cells, CD56+ CD16- CD57+ NK cell, CD56+ CD16+ CD57+ NK cells (Fig. S3).

Uniform Manifold Approximation and Projection (UMAP) was performed with uwot v0.1.14 (Melville, 2022) using CD3, CD4, CD8a, CD19, CD14, CD56, CD16 and CD57 normalized expression values of 10e5 randomly sampled events. Remaining events were subsequently projected onto the UMAP embedding. ggplot2 v3.4.0 (Hadley, 2016) was used for visualization.

For supervised analysis, cleaned fcs files were loaded in FlowJo 10.7.2 and the 15 cell populations of interest (see above) were manually gated. FlowJo workspace with manual gating information was then loaded into R using packages CytoML v2.10.0 (Finak et al., 2018) and flowWorkspace v4.10.0 (Finak, 2022). The Matthews Correlation Coefficient (MCC) was used to compare cell populations obtained with semi-automated analysis and manual gating for the FSFC data. For each cell population MCC = (TP*TN-FP*FN)/sqrt((TP + FP)*(TP + FN)*(TN + FP)*(TN + FN))) where TP, TN, FP and FN are the number of true positive, true negative, false positive and false negative cell assignment to the selected population by clustering, arbitrarily considering manually gated cell assignment as the gold-standard (MCC is invariant under the exchange of gold-standard) (Matthews, 1975).

3. Results

We first designed and built a 33-color antibody panel to comprehensively quantify major immune and NK cell subpopulations based on extra- and intracellular markers (Table S1, S2; Fig. S1, S2). This panel

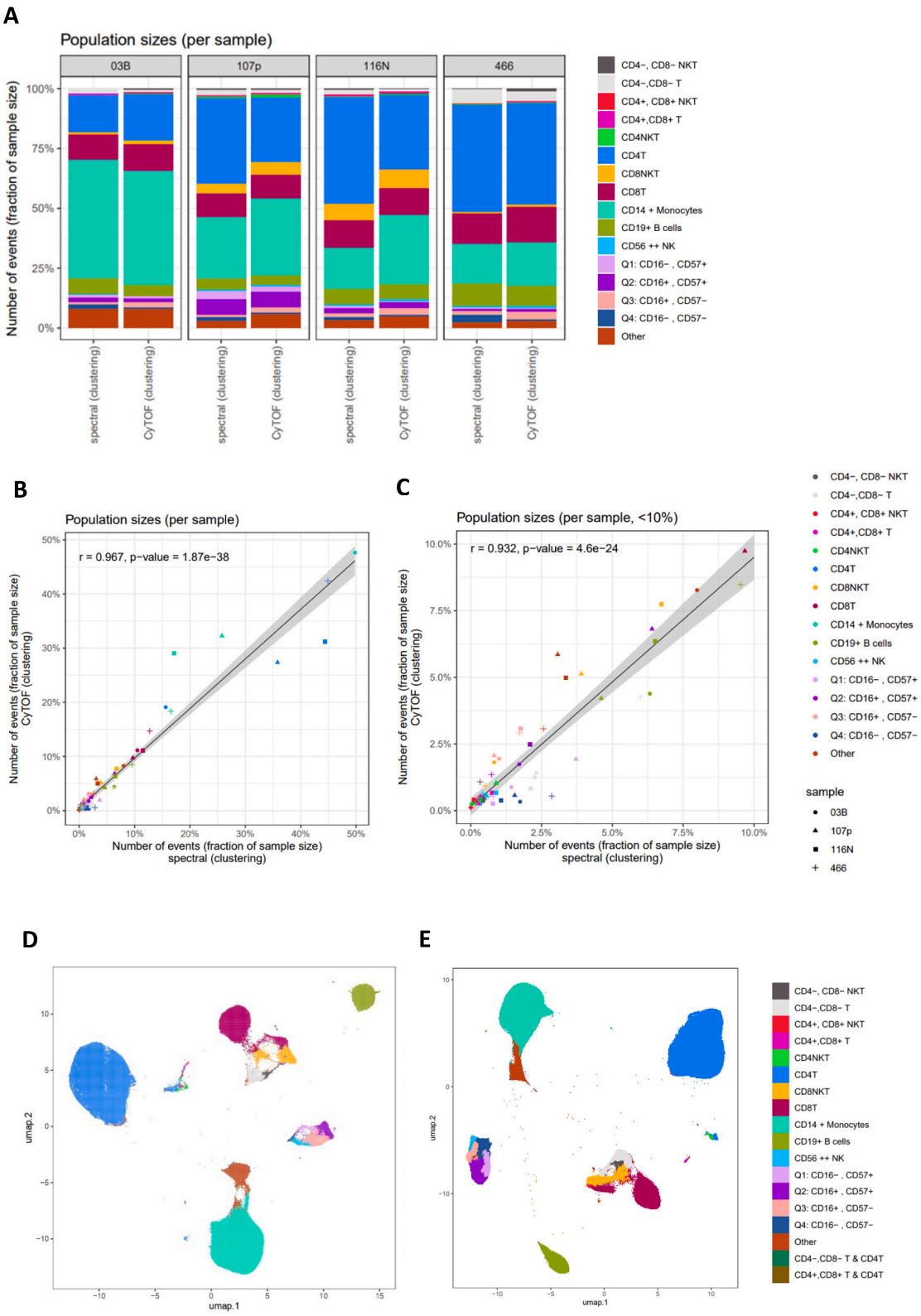

Fig. 1. Comparison between CyTOF and FSFC dataset. A. Abundances of 15 Cell populations identified with semi-automated analysis for the FCFS and CyTOF datasets across individual samples B. Comparison of cell population (color) abundances obtained with semi-automated analysis for the CyTOF (y-axis) and FCFS (x-axis) data sets, per sample (symbol). Linear regression line is shown in black with the 95% confidence interval (grey) C. Comparison of cell population (color) abundances limited to populations with abundance below 10% obtained with semi-automated analysis for the CyTOF (y-axis) and FCFS (x-axis) data sets, per sample (symbol) D. UMAP for the CyTOF data set, color-coded by cell population obtained with semi-automated analysis. Events are color - colored according to the 15 cell populations obtained with FlowSOM clustering. E. Same as for D for the FSFC dataset.

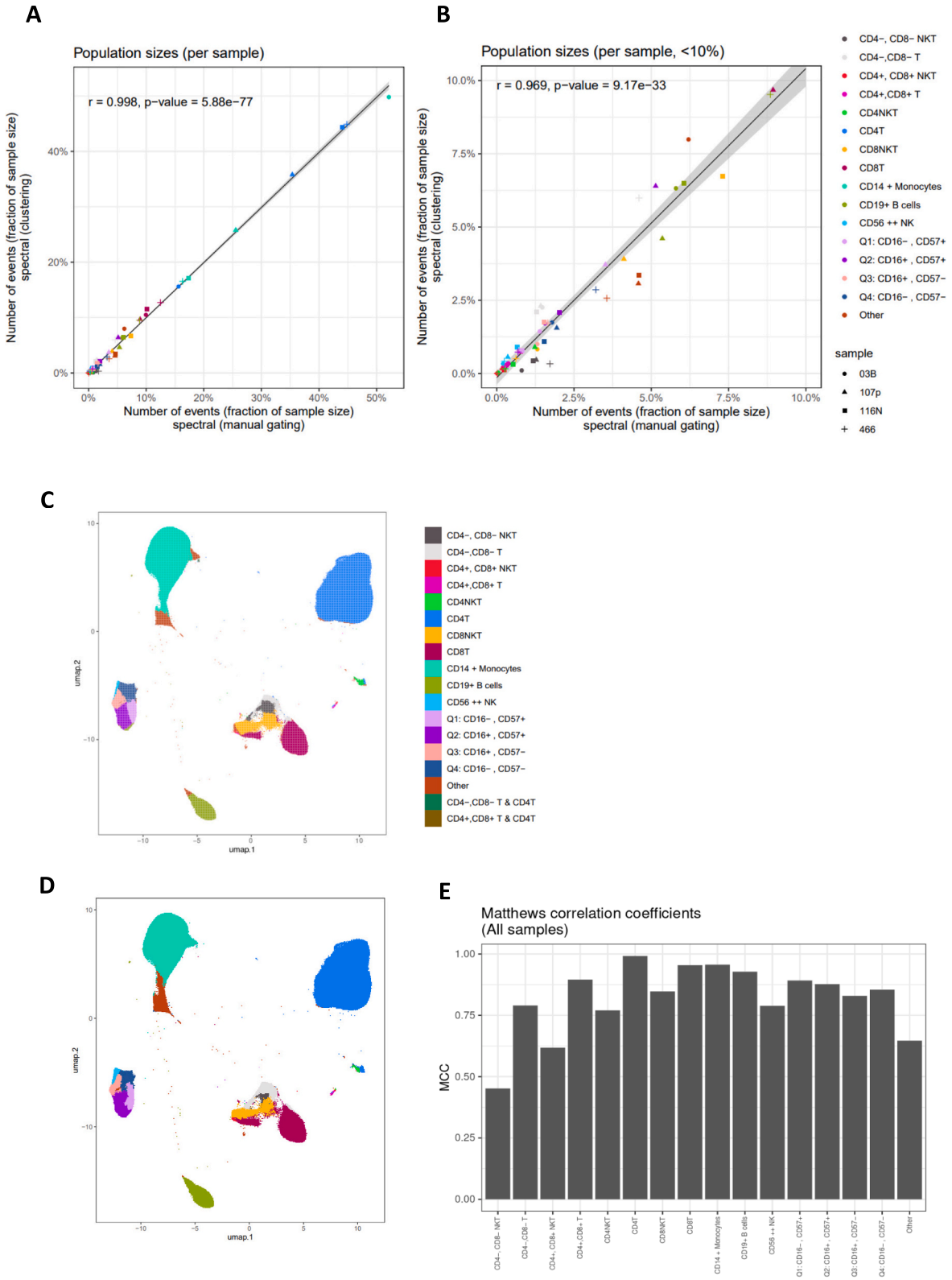

Fig. 2. Comparison between semi – supervised and supervised analysis in FSFC dataset. A. Comparison of cell population (color) abundances obtained with semi-automated analysis (y-axis) and manual gating (x-axis) for the FCFS data set, per sample (symbol). Correlation plots representative of the quantitative comparison (cluster frequencies) between FSFC and CyTOF for all 15 clusters identified by manual gating and FlowSOM clustering. Linear regression line is shown in black with the 95% confidence interval (grey). B. Comparison of cell population (color) abundances limited to populations with abundance below 10% obtained with semi-automated analysis (y-axis) and manual gating (x-axis) for the FCFS data set, per sample (symbol). C. UMAP for the FSFC data set. Events are color - colored according to the 15 cell populations obtained with manual gating. D. UMAP for the FSFC data set, color-coded by cell population obtained with semi-automated analysis. Events are color - colored according to the 15 cell populations obtained with FlowSOM clustering E. Comparison of cell populations obtained with manual gating and semi-automated analysis using Matthews Correlation Coefficient (MCC).

encompasses major NK cell receptor classes such as natural cytotoxicity receptors (NCRs), C-type lectin like receptors (NKG2) and activation marker such as perforin, granzyme B and CD107a (Pegram et al., 2011; Mahnke et al., 2015; Vanikova et al., 2022; Kay et al., 2016). To ensure that a relevant comparison of the technologies could be made, we developed the identical panel for full spectral flow cytometry and mass cytometry encompassing the exact same antibodies. Due to the limited availability of antibodies, identical clones could only be allocated to the same antibody for part of the panel. The panel development and validation strategy was performed as follows: (i) We allocated antibodies to fluorochromes by associating low expressed targets such as KIRs to brighter fluorochromes and high expressed targets such as lineages markers to dim fluorochromes (ii) We then proceeded to antibody titrations to ensure optimal staining patterns and minimize unspecific binding by calculating the appropriate concentration (iii) To accurately assess the positivity threshold of low expressed antigens and the specificity of the staining, we included a fluorescent-minus-one (FMO) control including following lineage markers: CD3, CD8a, CD4, CD19, CD14, CD56, CD16, CD57 (iv) We finally applied the full panel by staining non-stimulated and stimulated cryopreserved PBMCs derived from four healthy individuals.

Comparison of cell population abundances based on a semi-automated approach between CyTOF and FSFC.

We conducted the comparative study on PBMCs samples derived from four healthy individuals. Aliquots from each individual were equally labeled with the CyTOF panel and the FSFC panel prior to machine acquisition. We firstly wondered about the consensus between the two platforms in distinguishing major canonical immune cell subsets selecting eight basic lineage markers: CD3, CD4, CD8a, CD19, CD14, CD56, CD16, and CD57. We analyzed each dataset by a supervised immune clustering labelling step using semi-automated approach based on unsupervised clustering with FlowSOM followed by a supervised assignment of clusters into 15 cell types (see methods for details). With this approach, 95% of CyTOF events and 96% of FSFC events were assigned to a cell population and only the small remaining proportion could not be classified. Cell frequencies varied over a wide range, from 0.0039% to 52.1% per sample/per population. The frequency distribution of cell population abundance for each technique and sample is depicted in Fig. 1A.

The proportion of each cell population derived from the two techniques were highly concordant as reflected by the Pearson's correlation coefficient of $r = 0.967$ (p-value $= 1.9*10^{-38}$) stratified per cell population and per sample (Fig. 1B). As these correlative results can be biased by the presence of highly abundant cell populations, we next focused our analysis on low abundant cell populations comprising <10% of the total cell repertoire. Using the same approach, we revealed an overall high agreement ($r = 0.932$, p-value $= 4.6*10^{-24}$) between these platforms despite decreasing cell population abundance, further enhancing the data alignment between the two techniques (Fig. 1C).

In addition to the quantitative comparison, Uniform Manifold Approximation and Projection (UMAP) was used for dimension reduction for data structure visualization. UMAP plots of CyTOF (Fig. 1D) and FSFC (Fig. 1E) datasets show a remarkably similar distribution of cell subsets although not localized at the exact same localization. Some clusters populations were more delineated when looking at the FSFC dataset such as the CD16 -, CD57- NK cells and the CD4−, CD8− NKT subset than in the CyTOF dataset (Fig. 1D, E).

Comparison of cell population assignment between manual and automated approach based on the FSFC dataset.

There is an increasing tendency to shift towards more sophisticated automated or semi – automated methods to analyze and interpretate high-dimensional datasets that comes at a cost of data accuracy. Herein, we assessed the concordance of cell population assignment and quantification between the manual gating and semi-automated analysis for the newly emerged spectral flow cytometry technique. We manually gated the cells to assign them to the 15 clusters of interest defined previously and imported the dataset in R environment for downstream analysis. The agreement between both approaches was highly significant, reaching a correlation of $r = 0.998$ (p-value $= 5.88*10^{-77}$) for all cell populations (Fig. 2A) and $r = 0.969$ (p-value $= 9.17*10^{-33}$) for low frequent cell populations (<10%) (Fig. 2B). In line, UMAP plots of semi-automated and manual gated cell populations show a highly similar projection in terms of distance and localization (Fig. 2C, D).

We further thought to separately investigate the overlap between the different cell populations obtained with semi-automated and with manual gating by applying the Matthew's correlation coefficient (MCC). Analysis across all samples revealed accurate assignment for highly abundant population such as $CD4^+$, $CD8^+$, $CD19^+$ and $CD14^+$ cell population with a median matthew's correlation factor r above 0.9. Suboptimal scorings were found for small populations such as NK cell subsets and more drastically in NKT populations with the lowest correlation factor reaching 0.45 (Fig. 2E). We thus searched to quantify and investigate the origin of the non-concordant assignment of these populations based on a contingency table (Fig. S4). Enhanced leakages of cells were found between $CD4^+/CD8^+$ T cells and $CD4^+/CD8^+$ NKT subsets and in-between CD56/CD16/CD57 combinatorial NK subsets. This reflects the non-dichotomous staining pattern of these subsets leading to false cluster allocation with the potential to impact the downstream statistical analysis and biological interpretation (Fig. S4).

4. Discussion

The recently emerging mass cytometry and full spectrum flow cytometry techniques have greatly enhanced our capacity to probe biological systems at a high resolution and scalability with their capacity to measure several parameters simultaneously in one assay (Mahnke et al., 2015; Vanikova et al., 2022; Rahim, 2016; Chattopadhyay et al., 2019; Barcenilla et al., 2019; Horowitz et al., 2013). In clinical studies, samples are often derived from precious, limited and non-replaceable sources, frequently yielding low cell number. Thus, a thoughtful examination of the appropriate analysis tool needs to be undertaken to maximize data output. In this proof-of-concept study, we set out a biological comparative analysis of the two state-of-the art single cell proteomic technologies, cytometry by time-of-flight and full spectrum flow cytometry using an identical panel of 33 markers. Our results first revealed a high agreement between the two datasets in the quantification of major canonical immune cell subsets using a semi-automated computational approach and which is in concordance with recent findings (Ferrer-Font et al., 2020; Jaimes et al., 2022; Oetjen et al., 2018; Gadalla et al., 2019; van der Pan et al., 2023). Rare subpopulations showed minor disagreements between both techniques that can be attributed to their low frequency abundance and the acquired cell number.

The increasing number of bioinformatics tools emerging alongside the increasing output of biological data substantiate the need for validation of cell phenotypes and accuracy in assignment. While distinct populations with a clear separation of negative and positive such as $CD8^+$ T cells and $CD19^+$ B cells could be accurately captured by both semi-automated analysis and manual gating in our analysis, populations that were more subject to spreading such as NKT cells showed more discrepancies in the assignment. Thus, despite their explorative and multi-dimensional analysis ability, clustering tools (FlowSOM) bear the potential to over-estimate or under-estimate cell populations even with supposedly basic markers such as CD56 and CD16 and need to be applied with cautions for non-bimodal markers.

The choice of technology is highly dependent on the study design and not primarily on the biological output, as shown to be highly overlapping in our analysis. Indeed, each of these technologies have their strengths and weaknesses regarding their technical performance. With a theoretical acquisition of 100 parameters simultaneously and the minimal spillover inherent to the use of metal isotopes, Mass Cytometry represent a great tool to investigate the breadth of cellular systems

Table 1
Comparative assessment of technical, logistical and financial aspects between CyTOF and FSFC platforms (Bandura et al., 2009; Bendall et al., 2011; Leipold and Maecker, 2012; Maecker and Harari, 2015; Ornatsky et al., 2010).

Theme	Parameter	CyTOF	FSFC	Study
Technical	Number of parameters	43	40	How many samples are included? What is the timeframe of the study? Are rare subsets a special focus of the study? What kind of samples are included? According to the study design is there a possibility of barcoding?
	Throughput (cells/s)	500	10–15′000	
	i.e., 60 x 10^e6	*~ 30 h*	*~ 1, 5 h*	
	Cell transmission efficiency	30–60%	> 95%	
	Cell size/ complexity	No	Yes	Will there be several sample batches of acquisition? Pre – knowledge about the staining pattern of antibodies?
	Autofluorescence	No	Yes	
	Compensation	No	Yes	
	Sensitivity	300–400	< 40	
Logistical	Cell sorting	No	Yes	Are there specific clones that need to be considered?
	Panel flexibility	High	Medium	
	Panel extension	High	Limited	
	Antibody availability	Single vendor – in house conjugation	Many vendors – company customization	
	Training investment	High	Low	Is there a need of the samples to be freshly stained and acquired?
	Barcoding	Yes	No	
Financial	Antibody costs (100 tests, CHF)	550	300–600	What is the overall financial budget for the study?
	Infrastructure and maintenance costs	2 32 A plugs + Argon supply + Air extraction	MilliQ water +1 12 A plug	
	Data acquisition costs (1e^6 cells)	15 CHF	1–2 CHF	

CyTOF: Cytometry by time-of-flight, FSFC: Full spectrum flow cytometry.

without autofluorescence or the need to compensate spectral overlap (Kashima et al., 2022; Lo Tartaro et al., 2022). The minimal overlap between metal isotopes offers furthermore a higher flexibility in the translation and customization of panels then for spectral flow cytometry and which can be of great benefit in various clinical settings. However substantial constrains exist with the mass cytometry technique: slow acquisition speed, low cell throughput and it remains considerably expensive (Leipold and Maecker, 2012; Spitzer and Nolan, 2016). Full spectral flow cytometry is a direct response to these drawbacks, enabling acquisition of a large amount of data in reduced runtimes and with a considerably higher cell throughput (Chattopadhyay et al., 2019; Bonilla et al., 2020). Full spectral flow cytometry provides the greatest benefit in terms of time to cost efficiency which is very valuable in clinical studies encompassing a large amount of samples. It allows simultaneously to rapidly extract as much data as possible, essential when detecting and monitoring the frequency of rare subpopulations. Finally, full-spectrum flow cytometry now offers the possibility to sort sub-populations of cells for subsequent and future applications. We summarized key considerations and questions in Table 1 that needs to be consciously interrogated when setting out a new clinical study. In conclusion, both tools can interchangeably be used to capture single cell data from a biological perspective as set out by our comparative analysis. Both modalities are valuable and complementary tools on the market for addressing research questions in immunophenotyping studies.

Authors' contributions

A.S., S.D.: performed CyTOF and FSFC analysis and measurements. A.S., S.D., J.D.: performed the bioinformatic analysis. A.S.: drafted and wrote the manuscript. All authors revised and approved the final version for publication.

CRediT authorship contribution statement

Antonia Schäfer: Conceptualization, Investigation, Methodology, Writing – original draft. **Sènan Mickael D'Almeida:** Conceptualization, Investigation, Methodology, Software. **Julien Dorier:** Conceptualization, Methodology, Software. **Nicolas Guex:** Conceptualization, Methodology, Software. **Jean Villard:** Supervision, Validation, Writing – review & editing. **Miguel Garcia:** Conceptualization, Project administration, Supervision, Writing – review & editing.

Declaration of competing interest

All authors declare that there are no competing interests.

Data availability

Data will be made available on request.

Acknowledgements

We thank Juliette Desfrancois from Cytek and Emilie Gregori from Fluidigm for her support with the design of the antibody panels.

Appendix A. Supplementary data

Supplementary data to this article can be found online at https://doi.org/10.1016/j.jim.2024.113641.

References

Bandura, D.R., et al., 2009. Mass cytometry: technique for real time single cell multitarget immunoassay based on inductively coupled plasma time-of-flight mass spectrometry. Anal. Chem. 81 (16), 6813–6822.
Barcenilla, H., et al., 2019. Mass cytometry identifies distinct subsets of regulatory T cells and natural killer cells associated with high risk for type 1 diabetes. Front. Immunol. 10, 982.
Bendall, S.C., et al., 2011. Single-cell mass cytometry of differential immune and drug responses across a human hematopoietic continuum. Science 332 (6030), 687–696.
Bonilla, D.L., Reinin, G., Chua, E., 2020. Full Spectrum flow cytometry as a powerful Technology for Cancer Immunotherapy Research. Front. Mol. Biosci. 7, 612801.
Chattopadhyay, P.K., et al., 2019. High-parameter single-cell analysis. Annu Rev Anal Chem (Palo Alto, Calif) 12 (1), 411–430.
Ferrer-Font, L., et al., 2020. High-dimensional data analysis algorithms yield comparable results for mass cytometry and spectral flow cytometry data. Cytometry A 97 (8), 824–831.
Finak, G., . flowWorkspace: Infrastructure for representing and interacting with gated and ungated cytometry data sets. R package version 4.10.0. https://www.bioconductor.org/packages/release/bioc/html/flowWorkspace.html.
Finak, G., Jiang, W., Gottardo, R., 2018. CytoML for cross-platform cytometry data sharing. Cytometry A 93 (12), 1189–1196.

Futamura, K., et al., 2015. Novel full-spectral flow cytometry with multiple spectrally-adjacent fluorescent proteins and fluorochromes and visualization of in vivo cellular movement. Cytometry A 87 (9), 830–842.
Gadalla, R., et al., 2019. Validation of CyTOF against flow cytometry for immunological studies and monitoring of human Cancer clinical trials. Front. Oncol. 9, 415.
Hadley, W., 2016. ggplot2: Elegant Graphics for Data Analysis. Springer-Verlag, New York.
Hahne, F., et al., 2009. flowCore: a Bioconductor package for high throughput flow cytometry. BMC Bioinform. 10, 106.
Horowitz, A., et al., 2013. Genetic and environmental determinants of human NK cell diversity revealed by mass cytometry. Sci. Transl. Med. 5 (208), 208ra145.
Jaimes, M.C., et al., 2022. Full spectrum flow cytometry and mass cytometry: a 32-marker panel comparison. Cytometry A 101 (11), 942–959.
Kashima, Y., et al., 2022. Intensive single-cell analysis reveals immune-cell diversity among healthy individuals. Life Sci. Alliance 5 (7).
Kay, A.W., Strauss-Albee, D.M., Blish, C.A., 2016. Application of mass cytometry (CyTOF) for functional and phenotypic analysis of natural killer cells. Methods Mol. Biol. 1441, 13–26.
Leipold, M.D., Maecker, H.T., 2012. Mass cytometry: protocol for daily tuning and running cell samples on a CyTOF mass cytometer. J. Vis. Exp. 69, e4398.
Lo Tartaro, D., et al., 2022. Molecular and cellular immune features of aged patients with severe COVID-19 pneumonia. Commun. Biol. 5 (1), 590.
Maecker, H.T., Harari, A., 2015. Immune monitoring technology primer: flow and mass cytometry. J. Immunother. Cancer 3, 44.
Mahnke, Y.D., Beddall, M.H., Roederer, M., 2015. OMIP-029: human NK-cell phenotypization. Cytometry A 87 (11), 986–988.
Matthews, B.W., 1975. Comparison of the predicted and observed secondary structure of T4 phage lysozyme. Biochim. Biophys. Acta 405 (2), 442–451.
Melville, J., et al., 2022. Uwot: The Uniform Manifold Approximation and Projection (UMAP) Method for Dimensionality Reduction. R package version 0.1.14.
Nolan, J.P., Condello, D., 2013. Spectral flow cytometry. Curr. Protoc. Cytom. 1, 1.27.1–1.27.13.
Novo, D., Gregori, G., Rajwa, B., 2013. Generalized unmixing model for multispectral flow cytometry utilizing nonsquare compensation matrices. Cytometry A 83 (5), 508–520.
Oetjen, K.A., et al., 2018. Human bone marrow assessment by single-cell RNA sequencing, mass cytometry, and flow cytometry. JCI Insight 3 (23).
Ornatsky, O., et al., 2010. Highly multiparametric analysis by mass cytometry. J. Immunol. Methods 361 (1–2), 1–20.
Pegram, H.J., et al., 2011. Activating and inhibitory receptors of natural killer cells. Immunol. Cell Biol. 89 (2), 216–224.
R Core Team, 2022. R: A Language and Environment for Statistical Computing. R Foundation for Statistical Computing, Vienna, Austria. URL. https://www.R-project.org/.
Rahim, M.M., 2016. The downside of human natural killer cell diversity in viral infection revealed by mass cytometry. Ann. Transl. Med. 4 (24), 546.
Robinson, J.P., 2019. Spectral flow cytometry-quo vadimus? Cytometry A 95 (8), 823–824.
Robinson, J.P., 2022. Flow cytometry: past and future. Biotechniques 72 (4), 159–169.
Robinson, J.P., et al., 2012. Computational analysis of high-throughput flow cytometry data. Expert Opin. Drug Discov. 7 (8), 679–693.
Robinson, J.P., Li, N., Narayanan, P.K., 2015. High throughput-based mitochondrial function assays by multi-parametric flow cytometry. Curr. Protoc. Cytom. 73, p. 9 48 1-9 48 9.
Roederer, M., 2001. Spectral compensation for flow cytometry: visualization artifacts, limitations, and caveats. Cytometry 45 (3), 194–205.
Spitzer, M.H., Nolan, G.P., 2016. Mass cytometry: single cells. Many Features. Cell 165 (4), 780–791.
van der Pan, K., et al., 2023. Performance of spectral flow cytometry and mass cytometry for the study of innate myeloid cell populations. Front. Immunol. 14, 1191992.
Van Gassen, S., et al., 2015. FlowSOM: using self-organizing maps for visualization and interpretation of cytometry data. Cytometry A 87 (7), 636–645.
Vanikova, S., Koladiya, A., Musil, J., 2022. OMIP-080: 29-color flow cytometry panel for comprehensive evaluation of NK and T cells reconstitution after hematopoietic stem cells transplantation. Cytometry A 101 (1), 21–26.